

Effects of Atmospheric Humidity on the Refractive Index and the Size Distribution of Aerosols as Estimated from Light Scattering Measurements

By Tamio Takamura*, Masayuki Tanaka and Teruyuki Nakajima

Upper Atmosphere Research Laboratory, Tohoku University, Sendai 980, Japan

(Manuscript received 13 January 1984, in revised form 17 April 1984)

Abstract

The complex index of refraction, scattering cross section and albedo for single scattering have been estimated from measurements of the angular distribution of light scattered by aerosol particles, by an inversion library method. The humidity dependence of these optical properties has been examined in compiling 250 samples for the period February—November 1978. It is found that optical properties of aerosol particles change systematically according to the change of relative humidity. The humidity dependence of the complex index of refraction is explained by Hänel's theory introducing the mean mass increase coefficient for atmospheric aerosols consisting of both water-soluble and insoluble substances and the value of $1.58-0.04i$ for the complex index of refraction of dry particles.

Preliminary experiments of controlled relative humidity have also been performed to confirm the above results.

1. Introduction

Aerosol particles are produced from many different kinds of sources such as volcanic eruptions, wind erosions, industrial activities, organic activities and gas-to-particle conversion. Since the particles including hygroscopic substances are in thermodynamic equilibrium with surrounding moist air, their optical properties may be changeable with changing relative humidity. The extinction or scattering of light by aerosol particles have been studied theoretically or experimentally by many authors (e.g., Ahlquist and Charlson, 1969; Steinvall and Agren, 1975; Hänel, 1976; Patterson *et al.*, 1976; Bertolotti *et al.*, 1978; Pirich and Horvath, 1983). Recently, Okada and Isono (1982) have shown that the extinction coefficients deduced from the visibility data at Nagoya Local Meteorological Observatory depend strongly upon the relative humidity.

They suggested that the difference in the humidity dependence between 1960 and 1973 might be caused by different composition of aerosol particles as a result of the change in fuel usage from coal to oil.

In this paper, we discuss an average trend of the complex index of refraction, scattering cross section and albedo for single scattering in relation with the relative humidity. The original data used in this study have been obtained by analyzing the results of light scattering measurements for the wavelength of $0.5145 \mu\text{m}$ in the suburbs of Sendai by an inversion library method* (Tanaka *et al.*, 1982 and 1983). Just 250 samples for the period February—November 1978 are served for this study.

* This method has been newly developed, which simultaneously estimates the maximum likelihood values of the complex index of refraction and the size distribution of aerosol particles. It is assumed in the analysis that the aerosol particles are spherical and homogeneous.

* Present Affiliation: The National Defense Academy, Yokosuka, 239 Japan.

2. Application of the mixture rule

The humidity dependence of an uncharged aerosol particle is considered to be in thermodynamic equilibrium with the ambient moisture. Hänel (1976) has shown that the water activity of a pure solute a_w can be expressed as

$$a_w = \left(1 + \mu_s \frac{M_s}{M_w}\right)^{-1}, \quad (1)$$

where μ_s is the mass increase coefficient deduced from van't Hoff factor, M_s the mass of the solute and M_w the mass of water. The changes of the density ρ and the complex index of refraction m of the pure solute can be predicted from Eq. (1), if μ_s is known. The values of ρ and m depend upon the water activity through the mass of water uptake, and the water activity can be replaced by the equilibrium humidity f for a plane surface. Thus, increasing relative humidity decreases generally the particle density, and the complex index of refraction of the solute approaches that of water as relative humidity increases. Natural aerosol particles in a polydispersed system are, however, composed of various kinds of water-soluble and insoluble substances. The relationship between the water uptake per unit mass of dry matter and relative humidity is, therefore, assumed to be given by

$$\frac{M_w}{M_0} = \bar{\mu} \frac{f}{1-f}, \quad (2)$$

where $\bar{\mu}$ is the mean mass increase coefficient for the real aerosol particles composed of many substances, M_w and M_0 are masses of water and dry particles, respectively. The equation (2) means that an ensemble of the real aerosol particles is considered to behave like a large particle.

The mean value of the complex index of refraction of a polydispersed aerosol system can be obtained by applying the volume-weighted mixture rule to Eq. (2), as

$$m = m_w + (m_0 - m_w) \left(1 + \frac{\rho_0}{\rho_w} \bar{\mu} \frac{f}{1-f}\right)^{-1}, \quad (3)$$

where $m (=m_r - m_i \cdot i)$ is the mean value of the complex index of refraction of the polydispers-

sion in humid state, ρ_0 and m_0 are mean values of the density and complex index of refraction of dry particles, respectively, and ρ_w and m_w those of water. The validity of Eq. (3) have been examined by numerical simulations for several models of a two-component system. It is found that the optically equivalent value of m_r can be predicted fairly well by Eq. (3). On the other hand, the equivalent value of m_i cannot necessarily be predicted by the volume-weighted mean in Eq. (3). Similar results have also been found by Mita and Isono (1980) and Lederer *et al.* (1983) from comparisons for the single scattering albedo and the phase function, respectively. Results of our numerical simulation show that the equivalent value of m_i of the two-component system can be empirically approximated fairly well by the volume-weighted mean of the logarithm of m_i . We therefore adopt Eq. (3) for m_r , and the equation

$$\ln(m_i) = \ln(m_{iw}) - \ln(m_{i0}/m_{iw}) \cdot \left(1 + \frac{\rho_0}{\rho_w} \bar{\mu} \frac{f}{1-f}\right)^{-1}, \quad (4)$$

for m_i , substituting empirically $m_{iw} = 0.0015$ for $m_{i0} = 0^*$. Thus, if the mean values of m_0 , ρ_0 and $\bar{\mu}$ are known, one can estimate the values of m_r and m_i as functions of relative humidity. In addition, if the volume spectrum of aerosol particles is known, related optical quantities such as extinction cross section, scattering cross section, and albedo for single scattering can also be estimated as functions of relative humidity.

It is noted that the mean value of m_i estimated from Eq. (4) is considerably smaller than the equivalent value proposed by Mita and Isono (1980). This discrepancy is attributed to the fact that our method is based on reconstruction of the phase function (i.e. angular distribution of scattered light) instead of the albedo for single scattering by Mita and Isono (1980).

* Hänel and Dlugi (1977) have proposed an improved mixture rule for the imaginary part of the mean complex index of refraction. The mixture rule may overestimate the mean value of m_i compared with our results from Eq. (4) in the two-component system.

3. Results and discussions

3.1 Complex index of refraction

In order to obtain the humidity dependence of the complex index of refraction, 250 samples for the period February—November 1978 are classified into seven groups according to the value of relative humidity, as shown in Table 1. Figs. 1a and 1b show the mean value of m_r and m_i as functions of relative humidity, respectively. It is apparent that the mean values of m_r and m_i decrease systematically with an increase of the relative humidity. Since some differences are expected in the

Table 1 The mean values of the complex index of refraction for each humidity group. The column "cases" shows the number of measurements, m_r and m_i the real and imaginary parts of the complex index of refraction, respectively, and \bar{f} the mean value of relative humidity.

f	\bar{f}	cases	m_r	m_i
0—0.4	0.32	29	1.578	0.032
0.4—0.5	0.45	36	1.540	0.025
0.5—0.6	0.54	37	1.527	0.020
0.6—0.7	0.65	44	1.514	0.018
0.7—0.8	0.74	36	1.493	0.012
0.8—0.9	0.85	41	1.471	0.010
0.9—1.0	0.93	27	1.453	0.0091

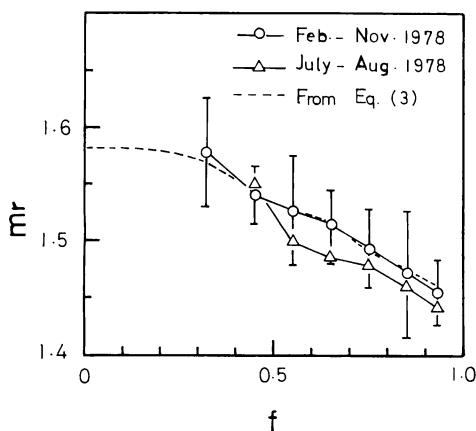


Fig. 1a The real part of the complex index of refraction versus relative humidity. The broken line shows the relation predicted from Eq. (3) using the mean value of the mass increase coefficient shown in Fig. 3. Vertical segments show the standard deviations of m_r for each humidity group.

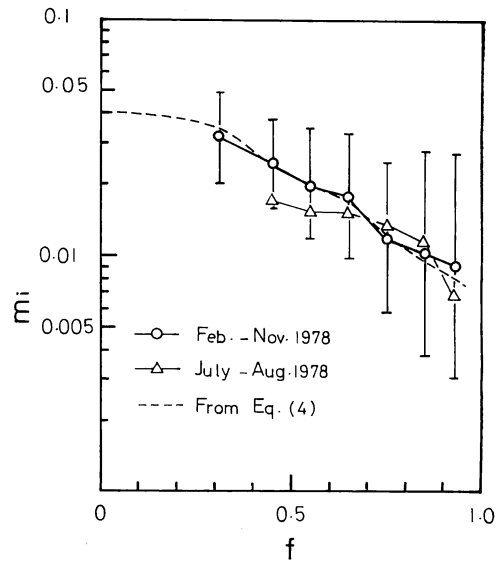


Fig. 1b The imaginary part of the complex index of refraction versus relative humidity. The broken line shows the relation predicted from Eq. (4). Vertical segments are the same as in Fig. 1a, but for m_i .

origin of aerosol particles between summer and other seasons due to different prevailing winds at the observation site, the data are also classified into July to August and other months. The value of m_r in summer months is slightly smaller than total average, as shown by triangles in Fig. 1a, but such a systematic trend is not seen in Fig. 1b for the value of m_i . As a whole, the difference between summer and other seasons is small as compared with large variability in respective seasons.

If the chemical composition of aerosol particles, and accordingly their optical constant, is modified mainly by the change of the relative humidity, the values of m_r and m_i have to exhibit a definite trend. In Fig. 2 is shown the relation of m_r vs m_i by open circles. If the complex index of refraction of aerosol particles obeys Eqs. (3) and (4), and relation between m_r and m_i should be expressed by a line segment the end points of which correspond to the complex indices of refraction of water and dry particles at the lower and upper limits, respectively. Though it is difficult to know precisely the values of $m_{r,0}$ and $m_{i,0}$ in dry state because of no chemical analyses in our programme, plausible values of $m_{r,0}$

and m_{i0} are estimated to be 1.58 and 0.04, respectively, from Figs. 1a, 1b and 2, the monthly variations of m_r and m_i (Tanaka *et al.*, 1982), and published results of Fischer (1970) and Hänel (1976). This value of m_0 is plotted in Fig. 2, by a cross symbol. The mean value of the mass increase coefficient $\bar{\mu}$ derived from Eqs. (3) and (4) using the above values of m_{r0} and m_{i0} and observed values of m_r and m_i . The values of $\bar{\mu}$ shown in Fig. 3 are obtained by averaging respective values of $\bar{\mu}$ for m_r and m_i . The particle density in dry state ρ_0 is assumed to be 2 and 3 g/cm³ from Hänel (1968, 1976) and Volz (1972). Though the absolute value of $\bar{\mu}$ is dependent upon the values of m_{r0} and m_{i0} , the trend is still kept similar to that shown in Fig. 3. The rapid increase of $\bar{\mu}$ around $f=0.4$ corresponds to the

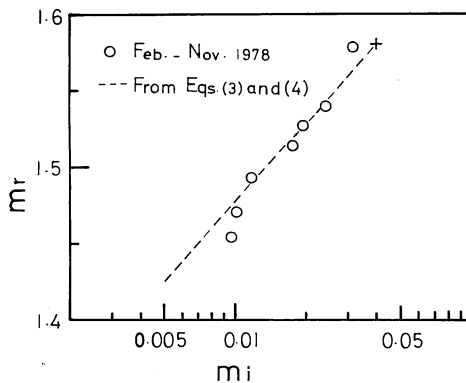


Fig. 2 The relation between the real and the imaginary parts of the complex index of refraction. The broken line shows the relation predicted from Eqs. (3) and (4), and cross the value of the complex index of refraction of dry particles assumed in this study.

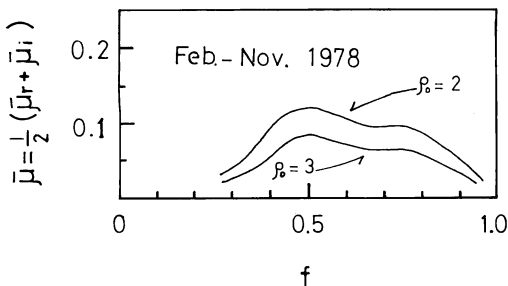


Fig. 3 The mean mass increase coefficient $\bar{\mu} = 1/2(\bar{\mu}_r + \bar{\mu}_i)$ versus relative humidity, for $\rho_0 = 2$ and 3 g/cm³. The complex index of refraction of dry particles is assumed to be $1.58 - 0.04i$.

sharp decrease of m , especially of m_r seen in Fig. 1a. Such a trend of the mass increase coefficient should be interpreted from chemical activities of the real particles for water vapor. Hänel (1976) has observed a sharp increase of $\bar{\mu}$ around $f=0.7$ for natural aerosols consisting of sea salt particles (Hänel's models 2 and 3). A rather flat trend of $\bar{\mu}$ similar to our results has also been found by Hänel (1976), for aerosols in Mainz region in summer season (Hänel's model 1). To interpret such behaviors of real aerosols and to evaluate the optical constant of dry particles more quantitatively, it is desirable to make chemical analyses simultaneously with scattering measurements, in the future. Broken lines in Figs. 1a, 1b and 2 show the values of m_r and m_i reconstructed from Eqs. (3) and (4) with above mentioned values of m_{r0} , m_{i0} and $\bar{\mu}$.

3.2 Scattering cross section and albedo for single scattering

The scattering cross section C_{sca} and the albedo for single scattering $\bar{\omega}_0$ can be obtained from the inferred size distribution $n(r)$ and complex index of refraction m , as follows:

$$C_{sca} = \int_{r_{min}}^{r_{max}} \pi r^2 Q_{sca}(m, \alpha) n(r) dr, \quad (5)$$

$$C_{ext} = \int_{r_{min}}^{r_{max}} \pi r^2 Q_{ext}(m, \alpha) n(r) dr, \quad (6)$$

and

$$\bar{\omega}_0 = C_{sca} / C_{ext}, \quad (7)$$

where $Q_{sca}(m, \alpha)$ and $Q_{ext}(m, \alpha)$ are scattering and extinction efficiency factors, respectively, α the size parameter, and r_{min} and r_{max} the minimum and maximum radii of particles contributing effectively to the measured angular distribution of scattered intensity within the range of scattering angle of $7^\circ \leq \theta \leq 170^\circ$ (Tanaka *et al.*, 1982). The values of 0.0384 and 3.41 μm are adopted for r_{min} and r_{max} , respectively, for the wavelength of 0.5145 μm . The scattering cross section C_{sca} and the albedo for single scattering $\bar{\omega}_0$ thus obtained are shown in Figs. 4 and 5, respectively. Both values of C_{sca} and $\bar{\omega}_0$ increase systematically with increasing relative humidity, except for the value of C_{sca} around $\bar{f}=0.74$

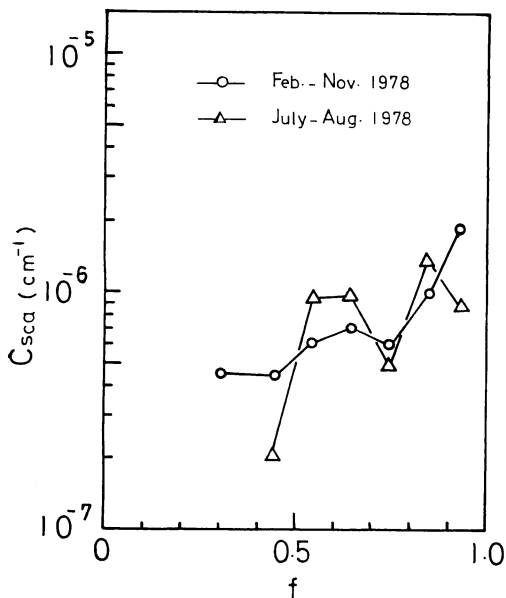


Fig. 4 The scattering cross section versus relative humidity. The values are calculated from the volume spectra shown in Fig. 7 for the wavelength of 0.5145 μm .

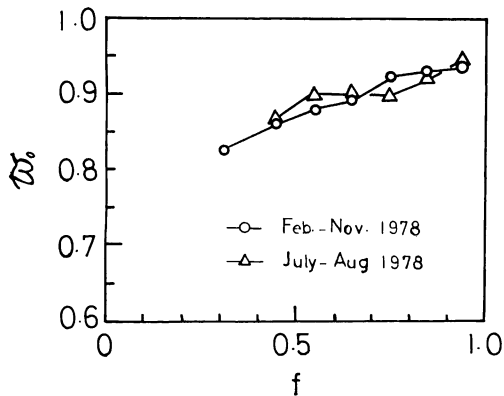


Fig. 5 The single-scattering albedo versus relative humidity. See caption to Fig. 4.

showing a slight decrease. These variations suggest that the optical properties of aerosol particles are modified according as the change of the relative humidity. Corresponding results for summer two months, July-Aug., are also shown in Figs. 4 and 5 by triangles. We can see again that there are no definite tendencies to characterize the difference between summer and other seasons. It is noted that the values of C_{sca} are more or less underestimated in proportion to the contribution of particles outside the effective range (i. e. $r >$

r_{max} and $r < r_{min}$).

The albedo for single scattering ω_0 is mainly dependent upon the imaginary part of the complex index of refraction. It is obvious that the correspondence of ω_0 with m_i is unique, if the size distributions for respective values of \bar{r} are unchanged within the effective size range. In order to examine this expectation, a size distribution of aerosols is assumed to obey a modified power law, as

$$n(r) \sim \text{constant} \quad \text{for } r_{min} \leq r \leq 0.1 \mu\text{m},$$

and

$$n(r) \sim r^{-(\beta+1)} \quad \text{for } 0.1 \mu\text{m} \leq r \leq r_{max},$$

where the exponent β is assumed to be 3.0 and 4.0 for models denoted by JNG-3 and JNG-4, respectively. Fig. 6 shows the relations between ω_0 and m_i calculated for JNG-3 and JNG-4 models and values of m_r of 1.45 and 1.55, comparing with observational results. The comparison between theoretical and observational results show that the size distribution of aerosols can be approximated by JNG-4 model, and that the likelihood value of the real part of the complex index of refraction decreases from 1.55 to 1.45 with increasing relative humidity.

The individual volume spectrum inferred by the inversion library method is averaged geometrically for respective groups of relative

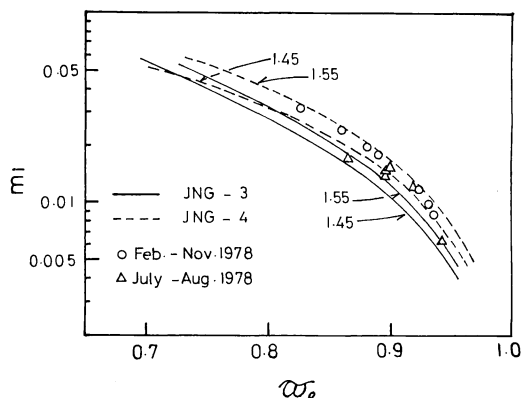


Fig. 6 The relation between the single-scattering albedo and the imaginary part of the complex index of refraction. Solid and broken lines correspond to the values of β of 3.0 (JNG-3) and 4.0 (JNG-4), respectively. Numerals attached to each line is the value of the real part of the complex index of refraction.

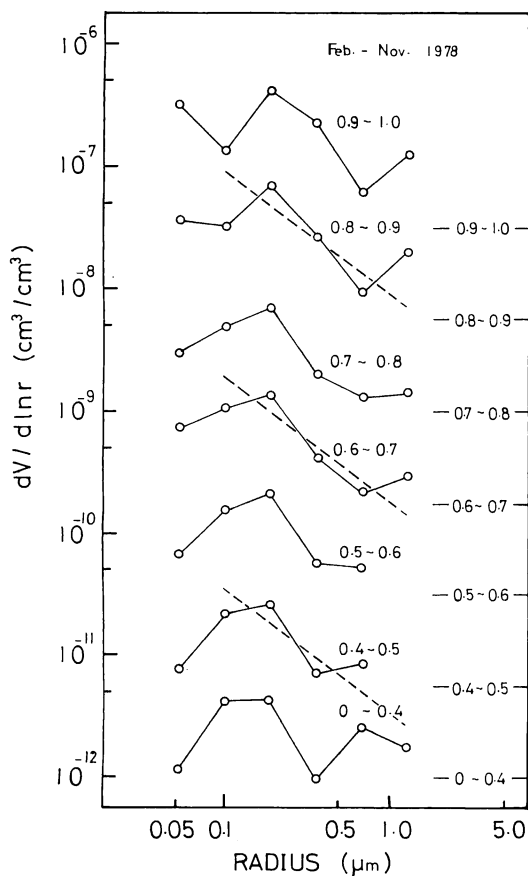


Fig. 7 The volume spectra of aerosol particles for respective humidity groups. Horizontal segments on the right side show the level $dV/dlnr = 10^{-12}$ to 10^{-11} cm^3/cm^3 for respective spectra, and broken lines the power-law distribution with $\beta = 4.0$.

humidity, as shown in Fig. 7. It is obvious that the retrieved spectra are close to the log-normal distribution rather than the power-law distribution. This is not contrary to the result of simulation shown in Fig. 6, because differences of the retrieved spectra from assumed power-law are not significant in the most important size range of $0.1 < r < 1.0 \mu\text{m}$ as shown by broken lines in Fig. 7. The mode radius of the volume spectrum increases only slightly as the relative humidity increases.

3.3 Results of experiments of controlled relative humidity

In the previous sections, mean optical properties of aerosol particles were presented in

relation with the relative humidity. Though these results are consistent with each other and seem to be reasonable from general considerations, uncertainty still remains because the air masses are different for different values of relative humidity. Therefore, it is of interest to confirm the results by controlling the relative humidity.

Aerosol samples introduced into a mixing tank (1.3 m^3 in volume) by a ventilating fan were mixed with water vapor prepared from a hot water vessel. It is not easy to supply air samples of well-controlled relative humidity for about 30 minutes by this method. Therefore, only a few examples obtained in stable states are reported here as preliminary results. The instrumental method used in the experiment was just the same as that for the measurements of the atmospheric aerosols for the period February–November 1978, except for the part of the humidifying process. The stability of the number density of aerosol particles during each measurement was also checked by a monitor detector at the scattering angle of about 30° . Results of this experiment are summarized in Table 2, where Case V shows the results for the experimental data of Quiney and Carswell (1972). The background data, indicated by “BG” in the last column of the table, were obtained for air samples introduced directly into the scattering volume without passing through the mixing tank.

Fig. 8a and 8b show the real and imaginary parts of the complex index of refraction as functions of the relative humidity. Arrows in these figures designate the direction of change, i.e. humidification or desiccation. It is noted that the most likelihood values of the complex index of refraction are selected stepwisely in the preliminary table of the complex index of refraction so that their uncertainties are rather large amounting to the grid size of the library of the complex index of refraction. As seen in Fig. 8a, the humidity dependence of the real part of the complex index of refraction is noticeable. The value of m_r reaches 1.35 in the final stage of humidification in Case IV, being very close to that of water. The corresponding behavior

Table 2 Summary of the experiments of controlled relative humidity. The values of the scattering and extinction cross sections, C_{sca} and C_{ext} are estimated from the volume spectra for optically effective range of the particle size.

Case	Date 1978	Time	Temp (C)	f	m_r	m_i	C_{sca} (cm ⁻¹)	C_{ext}	$\tilde{\omega}$	Note
I	5/3	12:18-12:53	17.8	0.20	1.60	0.05	3.67E-7	4.93E-7	0.75	B G
		16:48-17:30	28.0	0.67	1.50	0.03	1.68E-6	2.03E-6	0.82	
		18:22-19:08	26.7	0.90	1.40	0.03	1.36E-5	1.82E-5	0.75	
II	8/24	15:50-16:30	25.0	0.41	1.60	0.03	1.47E-7	2.23E-7	0.66	B G
		18:02-19:30	37.3	0.79	1.45	0.03	1.33E-6	2.18E-6	0.61	
III	8/25	16:30-17:10	41.0	0.95	1.40	0.01	1.45E-6	1.79E-6	0.81	B G
		17:29-18:02	23.0	0.70	1.50	0.01	3.45E-7	4.43E-7	0.78	
IV	9/1	11:56-12:29	18.4	0.84	1.50	0.02	4.41E-7	5.09E-7	0.87	B G84
		14:15-14:50	33.9	0.37	1.55	0.03	3.50E-7	4.27E-7	0.82	R H37
		16:00-17:00	33.5	0.90	1.40	0.005	2.60E-6	2.80E-6	0.93	R H90
		17:45-18:25	50.0	0.98	1.35	0.005	9.99E-6	1.07E-5	0.94	R H98
V	Quiney & Carswell (1972)			0.77	1.50	0.02			0.84	
				0.86	1.45	0.02			0.85	
				0.90	1.40	0.01			0.86	
				0.95	1.40	0.01			0.88	
				0.99	1.34	0.0			1.0	

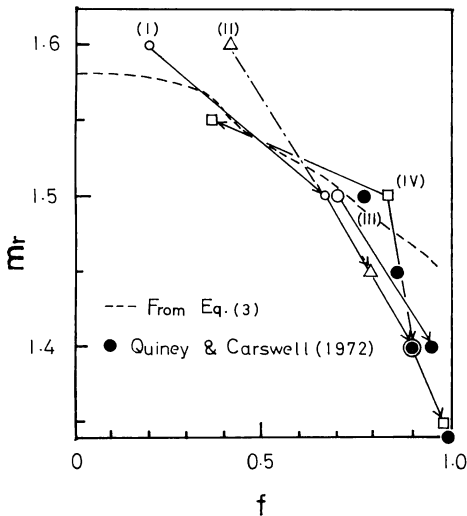


Fig. 8a The real part of the complex index of refraction versus relative humidity. The broken line is the same one as in Fig. 1a. Roman numerals correspond to the cases given in the first column of Table 2.

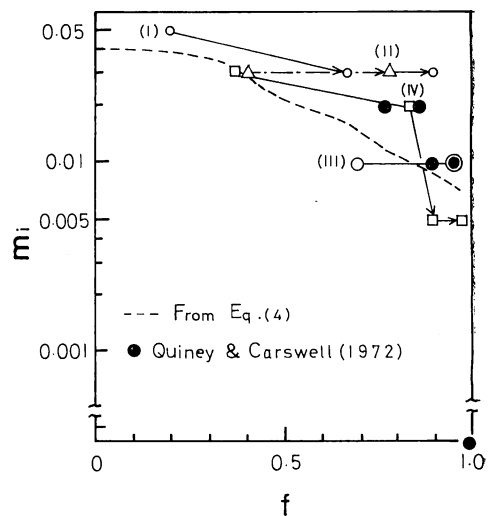


Fig. 8b The imaginary part of the complex index of refraction versus relative humidity. The broken line is the same one as in Fig. 1b. See caption to Fig. 8a.

of the imaginary part is similar to that of the real part, but the humidity dependence is less distinctive than the real part (Fig. 8b). This may be caused by the fact that the inversion library method has higher sensitivity for m_r than for m_i (Tanaka *et al.*, 1982). In Figs. 8a and 8b are also shown the humidity dependences of m_r and m_i predicted from Eqs. (3) and (4), respectively, by broken lines. The results of the humidity-controlled experiments are, generally, in fairly good agreement with the mean trend for natural aerosols shown in Figs. 1a and 1b.

Quiney and Carswell (1972) have reported the results of light scattering measurements similar to ours. Their data were also analyzed by our inversion library method. The results are shown in Figs. 8a and 8b by solid circles. Both of the real and imaginary parts of the complex index of refraction decrease rapidly as relative humidity increases from 0.77 to 0.99. The values of m_r and m_i at $f=0.99$ are found to be 1.34 and 0.0, just the same values as for pure water. These results strongly suggest that the target samples of their measurements were particles growing by accretion of water vapor. Of interest is that the results for Quiney and Carswell's measurements show a tendency very similar to our results, though in their experiments giant nuclei were filtered out leaving only particles less than $0.3 \mu\text{m}$ in diameter at the low relative humidity.

The growth of particles with increasing relative humidity in the optically effective range of particle sizes can be inferred from corresponding increase of the scattering cross section C_{sca} , as well as direct particle sizing. Fig. 9 shows the values of C_{sca} as a function of relative humidity. The broken line in the figure shows the average trend of atmospheric aerosols for the period February—November 1978. The increase of the value of C_{sca} due to humidification is noticeable, as compared with the mean behavior of natural aerosol particles. It seems to correspond to smaller values of m_r than the average trend for the period February—November 1978, as shown in Fig. 8a. This discrepancy may be attributable, at least partly, to our method of

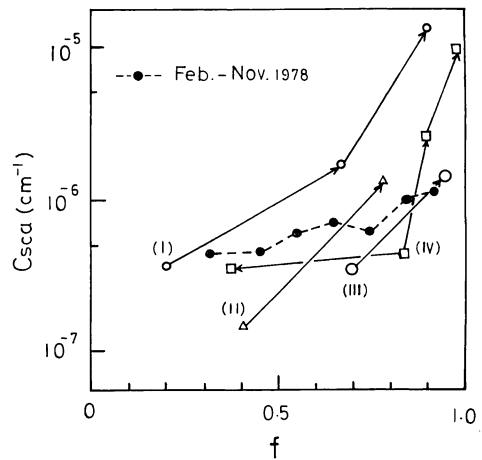


Fig. 9 The scattering cross section versus relative humidity. The broken line shows the mean trend for the period February—November 1978. See caption to Fig. 8a.

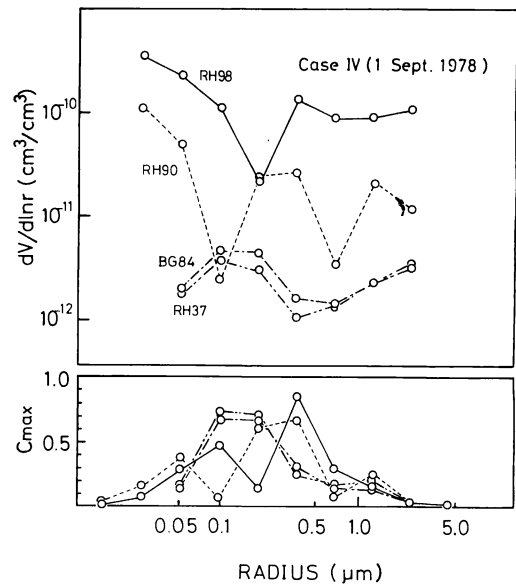


Fig. 10 The volume spectra and corresponding maximum contribution index C_{max} for Case IV of the humidification experiments.

humidification. A temporary supersaturation occurs in the neighborhood of water-vapor source in our experiment, and some hydrophilic particles are expected to grow up.

The change of the volume spectrum due to humidification (or desiccation) is shown in Fig. 10 for Case IV, where C_{max} is the maximum contribution of a given spectral portion to any portion of the phase function (i.e.

original data) (Tanaka *et al.*, 1982). As seen in the figure, the volume spectrum grows noticeably and the most effective size corresponding to the maximum value of C_{\max} increases from 0.1 to 0.4 μm , as relative humidity increases from 0.37 to 0.98. Such a change of the volume spectrum due to humidification is larger than that of the mean volume spectrum shown in Fig. 7. This feature may be reflected in somewhat small values of $\bar{\omega}_0$ found in the humidification experiment, as seen in Table 2.

Acknowledgements

This paper is dedicated to Prof. G. Onishi of the National Defense Academy with authors' sincere thanks for his encouragement. This study was supported by Research Project, Grant in Aid for Scientific Research of the Ministry of Education, Science and Culture, Japan, Project Number 446037.

References

- Ahlquist, N. C. and R. J. Charlson, 1969: Measurement of the wavelength dependence of atmospheric extinction due to scatter. *Atmospheric Environment*, **3**, 551-564.
- Bertolotti, M., M. Carnevale and D. Sette, 1978: Atmospheric extinction measurement of a He-Ne laser. *Appl. Opt.*, **17**, 285-288.
- Fischer, K., 1970: Measurements of absorption of visible radiation by aerosol particles. *Beitr. Phys. Atmosph.*, **43**, 244-254.
- Hänel, G., 1968: The real part of the mean complex refractive index and the mean density of samples of atmospheric aerosol particles. *Tellus*, **20**, 371-379.
- , 1976: "The properties of atmospheric aerosol particles as functions of the relative humidity at thermodynamic equilibrium with the surrounding moist air.", *Adv. Geophys.*, vol. 19, Academic Press, New York, 73-188.
- and R. Dlugi, 1977: Approximation for the absorption coefficient of airborne atmospheric aerosol particles in terms of measurable bulk properties. *Tellus*, **29**, 75-82.
- Lederer, L., H. Quenzel and E. Thomalla, 1983: The usefulness of a bulk refractive index for the calculation of the scattering properties of mixtures of aerosol particles at wavelength 530 nm. *Beitr. Phys. Atmosph.*, **56**, 94-107.
- Mita, A. and K. Isono, 1980: Effective complex refractive index of atmospheric aerosols containing absorbing substances. *J. Meteor. Soc. Japan*, **58**, 69-80.
- Okada, K. and K. Isono, 1982: Trends in visibility in the urban atmosphere —A case study in Nagoya, Japan—. *J. Meteor. Soc. Japan*, **60**, 777-786.
- Patterson, E. M., D. A. Gillette and G. W. Grams, 1976: The relation between visibility and the size-number distribution of airborne soil particles. *J. Appl. Meteor.*, **15**, 470-478.
- Pirich, R. and H. Horvath, 1983: On the influence of meteorological parameters on extinction and mass size distributions in the urban aerosol of Vienna. *Beitr. Phys. Atmosph.*, **56**, 84-93.
- Quiney, G. and A. I. Carswell, 1972: Laboratory measurements of light scattering by simulated atmospheric aerosols. *Appl. Opt.*, **11**, 1611-1618.
- Steinvall, Ove and C. H. Agren, 1975: Measurements of atmospheric extinction in the spectral region 360-800 nm by spectroradiometry. *J. Appl. Meteor.*, **14**, 603-608.
- Tanaka, M., T. Nakajima and T. Takamura, 1982: Simultaneous determination of complex refractive index and size distribution of airborne and water-suspended particles from light scattering measurements. *J. Meteor. Soc. Japan*, **60**, 1259-1272.
- , T. Takamura and T. Nakajima, 1983: Refractive index and size distribution of aerosols as estimated from light scattering measurements. *J. Climate Appl. Meteor.*, **22**, 1253-1261.
- Volz, F. E., 1972: Infrared absorption by atmospheric aerosol substances. *J. Geophys. Res.*, **77**, 1017-1031.

エアロソルによる散乱光から推定される 複素屈折率及び粒径分布の湿度依存性

高村民雄*・田中正之・中島映至

東北大学理学部超高層物理学研究施設

エアロソルによる散乱光強度の角度分布の情報から、エアロソルの複素屈折率及び粒径分布が、Inversion-library法を用いて、求められてきた。ここでは、1978年2月から11月に至る、仙台・青葉山での250の観測例から、これらの粒子の光学的性質の湿度依存性についてまとめた。

この期間のデータを一定の湿度範囲毎に分類してみると、エアロソルの光学的性質に、湿度に対する顕著な依存性のあることが明らかとなった。この依存性を説明する為に、Hänel の理論を適用した。この時、粒子の乾燥状態での複素屈折率を $1.58 - 0.04i$ とし、質量増加係数を屈折率の観測値から推定した。この値は、これまでの他の結果と比較して、妥当なものである。

これらの結果を確認する為に、実際の大気を用いて、数例の加湿実験を行なった。その結果は、2月から11月までの観測から得られた傾向を支持するものであった。

* 現所属：防衛大学校